Bull Volcanol (2009) 71:401–408
DOI 10.1007/s00445-008-0229-7

RESEARCH ARTICLE

Simulations of measures to control lava flows

Eisuke Fujita · Masataka Hidaka · Akio Goto · Susumu Umino

Received: 13 September 2007 / Accepted: 11 June 2008 / Published online: 16 July 2008

Abstract We evaluated the quantitative effects of artificial barriers, water-cooling and guiding channels on lava flow using the lava simulation program LavaSIM. Lava flow is basically subject to the topography around the path, effusive rate and viscosity. To prevent damage due to lava flow, we conducted experiments in controlling the flow direction, velocity and temperature. The simulation demonstrated that artificial barriers can successfully change the direction of a lava flow and is more effective when placed nearly parallel to the flow direction at a point where the topography is not very steep, while a barrier placed perpendicular to the flow direction can only stop the flux temporarily, ultimately allowing the solidified crust to accumulate and causing the following mass to go over the barrier. The water-cooling trial was also effective in controlling the direction and temperature, although the amount of water was as much order as 10^5 m^3. The guiding channels successfully control the direction and inundated area but only in local areas.

Keywords Lava flow · Numerical simulation · Artificial barrier · Water cooling · Guiding channels · Lava flow control · Solidification · Crust

Editorial responsibility: S. Nakada

E. Fujita (✉)
National Research Institute for Earth Science
and Disaster Prevention,
Tennodai 3-1,
Tsukuba, Ibaraki 305-0006, Japan
e-mail: fujita@bosai.go.jp

M. Hidaka
Power and Industrial Systems R D Laboratory, Hitachi, Ltd.,
7-2-1, Omika-cho,
Hitachi, Ibaraki 319-1221, Japan

A. Goto
Center for Northeast Asian Studies, Tohoku University,
41 Kawauchi, Aoba-ku,
Sendai, Miyagi 980-8576, Japan

S. Umino
Graduate School of Natural Science and Technology,
Kanazawa University,
Kakuma-cho, Kanazawa,
Ishikawa 920-1192, Japan

Introduction

Flow of lava is one of the significant surficial phenomena associated with volcanic eruptions, damaging environments and causing human death and injury. Compared with other phenomena like pyroclastic falls, it is possible to control lava flow, since lava is mainly subject to the local topography. Many attempts have been made to control the direction and the spread of lava flow using artificial barriers and channels, explosives, bombs, water cooling, and so on. The first trial, conducted at Etna, Italy, in 1669, attempted to change the direction of flow using barriers in order to protect the town of Catania (Cardaci 2004). Well-planned projects aiming to stop or control lava flow were carried out using artificial barriers and channels in 1983, 1991–1993 and 2001. In 1992, a barrier 21 m in height and 234 m in length with a total volume of soil and rocks of 3.7×10^5 m^3 was established in 10 days (Barberi et al. 1993; Vassale 1994; Barberi and Carapezza 2004). This was effective in restraining the flow for about 1 month, but the lava ultimately overflowed. Three additional barriers placed downstream were 6 to 12 m in height and 90 to 160 m in length. Explosives were placed to destroy the barrier and were successful in redirecting the natural flow into the artificial channels (Barberi et al. 1993; Barberi and Carapezza 2004).

In Hawaii, during the 1935 and 1942 eruptions, a 275 kg bomb was used to destroy the roof of a lava tunnel (Kauahikaua 2004), but these trials were not so effective. Trials using barriers were also conducted in 1955, 1960, 1977, 1984, and 2002.

Water-cooling is also an effective way to control lava flow. The most famous and successful water-cooling trial was conducted during the 1973 eruption of the Eldfell volcano on Heimaey Island, Vestmannnaeyjar, Iceland (Siguresirsson 1997). When the lava flow approached the seashore, the edge of the flow was continuously cooled by water, producing natural ramparts that changed the direction of flow. Also, based on their experience of water jets, the experimenters determined that the efficiency of water cooling is such that each cubic meter of water cools about 0.7 m^3 of lava, reducing the lava surface temperature by 100°C. Water cooling is more effective when it penetrates to the inner lava through cracks and joints that form during the initial cooling phase. But water cooling has a fundamental problem because lava has very low heat conductivity, so this trial required a huge amount of water from a source such as a reservoir and/or rivers.

For the assessment of these counteraction attempts, numerical simulations of lava flow can provide much useful information. A variety of simulation codes exist, and they are basically classified into two categories, probabilistic and deterministic (Costa and Macedonio 2005). The former is useful especially for quick evaluation of risky areas (e.g., DOWNFLOW by Favalli et al. 2005; FLOWFRONT by Wadge et al. 1994; SCIARA by Crisci et al. 2004). For more quantitative evaluation for counteraction projects, the deterministic models are preferable, since they can simulate physical phenomena including 3D convection, solidification and so on. In this paper, we evaluate the quantitative effects of artificial barriers, water cooling and guiding channels in controlling lava flow, based on a deterministic numerical simulation.

Lava flow simulation program: LavaSIM

Hidaka et al. (2005) developed a deterministic lava flow simulation program called LavaSIM that formulates three-dimensional flow by solving the Navier–Stokes equation, the energy equation, and the equation of continuity, with a free-surface evaluation, including boundary transport between the melt and the crust. The mass conservation is,

$$\frac{\partial u}{\partial x}+\frac{\partial v}{\partial y}+\frac{\partial w}{\partial z}=0, \tag{1}$$

where u, v and w are the velocity in x, y and z directions. The momentum conservation is,

$$\begin{aligned}&\frac{\partial u}{\partial t}+u\frac{\partial u}{\partial x}+v\frac{\partial u}{\partial y}+w\frac{\partial u}{\partial z} \\ &=\frac{1}{\rho}\left[-\frac{\partial P}{\partial x}+\frac{\partial}{\partial x}\left(\mu\frac{\partial u}{\partial x}\right)+\frac{\partial}{\partial y}\left(\mu\frac{\partial u}{\partial y}\right)+\frac{\partial}{\partial z}\left(\mu\frac{\partial u}{\partial z}\right)\right] \\ &-g\sin^2\theta\cos^2\phi\frac{\partial H}{\partial x},\end{aligned} \tag{2}$$

$$\begin{aligned}&\frac{\partial v}{\partial t}+u\frac{\partial v}{\partial x}+v\frac{\partial v}{\partial y}+w\frac{\partial v}{\partial z} \\ &=\frac{1}{\rho}\left[-\frac{\partial P}{\partial y}+\frac{\partial}{\partial x}\left(\mu\frac{\partial v}{\partial x}\right)+\frac{\partial}{\partial y}\left(\mu\frac{\partial v}{\partial y}\right)+\frac{\partial}{\partial z}\left(\mu\frac{\partial v}{\partial z}\right)\right] \\ &-g\sin^2\theta\sin^2\phi\frac{\partial H}{\partial y},\end{aligned} \tag{3}$$

$$\begin{aligned}&\frac{\partial w}{\partial t}+u\frac{\partial w}{\partial x}+v\frac{\partial w}{\partial y}+w\frac{\partial w}{\partial z} \\ &=\frac{1}{\rho}\left[-\frac{\partial P}{\partial z}+\frac{\partial}{\partial x}\left(\mu\frac{\partial w}{\partial x}\right)+\frac{\partial}{\partial y}\left(\mu\frac{\partial w}{\partial y}\right)+\frac{\partial}{\partial z}\left(\mu\frac{\partial w}{\partial z}\right)\right] \\ &-g\cos^2\theta\frac{\partial H}{\partial z}+K,\end{aligned} \tag{4}$$

where P, μ, H, θ, ϕ and K are the pressure, viscosity, sum of liquid head and ground elevation, ground inclination angle, the azimuthal direction of maximum ground inclination and external force, respectively. The energy conservation is

$$\begin{aligned}&\frac{\partial h}{\partial t}+u\frac{\partial h}{\partial x}+v\frac{\partial h}{\partial y}+w\frac{\partial h}{\partial z} \\ &=\frac{1}{\rho}\left[\frac{\partial}{\partial x}\left(\lambda\frac{\partial T}{\partial x}\right)+\frac{\partial}{\partial y}\left(\lambda\frac{\partial T}{\partial y}\right)+\frac{\partial}{\partial z}\left(\lambda\frac{\partial T}{\partial z}\right)\right]+Q,\end{aligned} \tag{5}$$

where h, λ, T and Q are the specific enthalpy, the thermal conductivity, temperature and heat transfer due to cooling at the surface and bottom, and between solid and liquid lava, respectively. This scheme can express not only the distribution and thickness of the lava flow but also detailed structures such as the convection inside the flow, and the melting and re-melting of the crust.

Our approach to solving these equations directly is somewhat time-consuming compared with schemes focusing on the flow distribution using cellular automata (e.g., Crisci et al. 2004) or the steepest path (e.g., Favalli et al. 2005), which are very effective for a quick, rough evaluation of lava flow damage. However, we have chosen to emphasize the physical processes of solid–liquid thermal fluid dynamics. In this paper, we simulate lava-flow control

using artificial barriers, water-spray cooling and guiding channels, in which the evaluation of heat transfer between the lava and other materials (atmosphere, water and structures) is the key to characterizing the lava-flow patterns.

Case study: 1986 Izu-Oshima eruption lava flow

Observation and simulation

Izu-Oshima is located about 120 km south of Tokyo (Fig. 1a). The 1986 eruption originated in the summit crater, with lava flows LA I–IV and LB I–II, which flowed inside the summit caldera. The eruption from the C-craters, located on the northwest flank outside the caldera rim, began 6 days after the initial stage. Figure 1b shows the distribution of the LC-I lava flow (Geographical Survey Institute 2006). A C-crater row began to open around 1745 local time (LT) on November 21, and the fire fountain continued for about 3 h. The LC-I lava flow began to run down the slope from the C6 crater around 1801 LT and almost came to a stop around 2400 LT. Unfortunately, the temporal evolution of the flow was not clear because the activity occurred during the night. However, one report indicated that the lava reached an altitude of 170 m around 1900 LT (Endo et al. 1988). Lava flow characteristics depend mainly on the viscosity, temperature, and emission rate, as well as on the topography of the flow area. Initially, we formulated the LC-I lava flow with no barriers or water-cooling in order to determine appropriate values for these important parameters (Fig. 1c). For the emission rate, we assumed 44 m^3/s, estimated using photogrammetric data and the duration of eruptions (Nagaoka 1988; Hayakawa and Shirao 1998; Ishihara et al. 1988). The lava flow stops when the thickness of the flow becomes less than the minimum threshold defined by the yield strength. Viscosity mainly governs lava movement and depends on the chemical composition and temperature of the molten lava; LavaSIM can simulate both effects. After trying various values for the viscosity, we adopted a constant value of 5.0×10^3 Pa s, with a view to matching the total lengths of the lava flow from the observation and the simulation. For example, for 1.0×10^4 Pa s, the final length of the simulated lava flow was about 70% of the observed value (Geographical Survey Institute 2006; Nagaoka 1988). In this paper, we use a constant effective viscosity, i.e., the viscosity does not change with the temperature as a preliminary trial, since the lava flow of LC-I was very fast and temporal change of viscosity can be approximated by the averaged value. The cell size was 10 m×10 m×1 m, the extrusion rate at the crater was 44 m^3/s (that is, 1.1×10^5 kg/s when we assume the density is 2.5×10^3 kg/m^3) until 3,600 s, the lava specific enthalpy was 1.2328×10^6 J/kg,

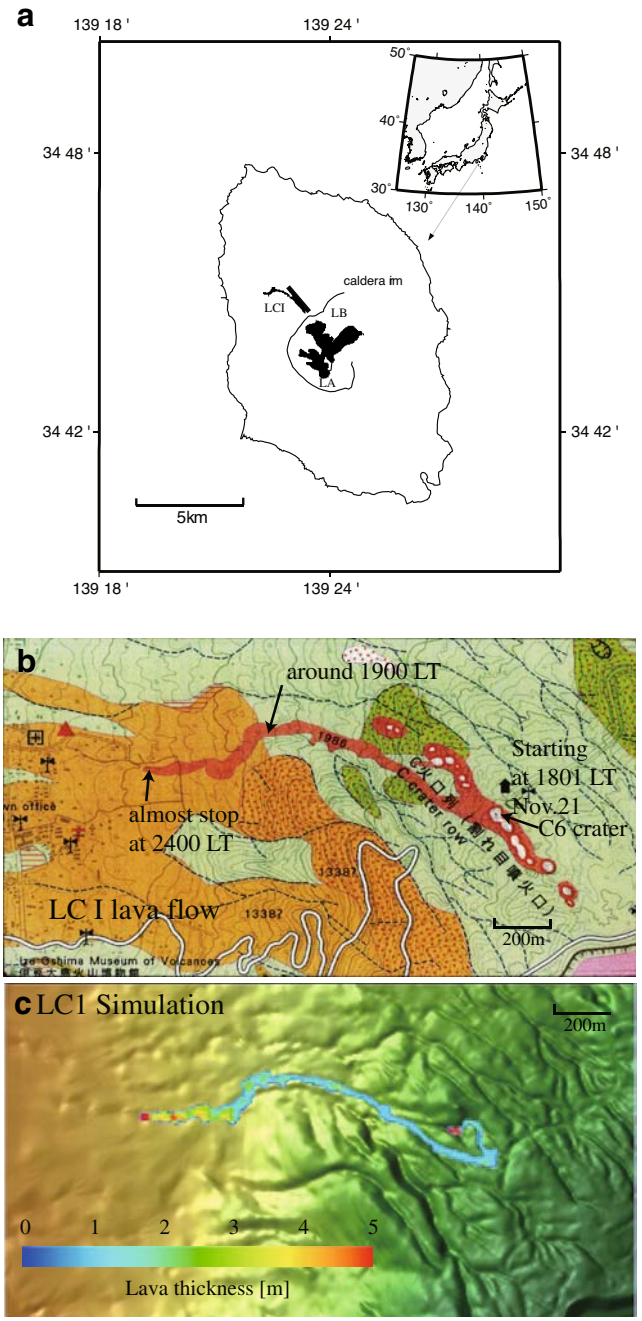

Fig. 1 **a** Location of Izu-Oshima volcano, Japan. The 1986 Izu-Oshima eruption is characterized by three major lava flows, LA, LB and LCI. **b** The observed lava flow LC I was emitted from the C6 crater at 1801 local time, Nov. 21. It flowed down the valley and turned to the south about 1900. The flow almost stopped at 2400, less than 200 m to a residential area. **c** The simulated lava flow using LavaSIM. Overall feature is well reproduced

the extrusion temperature was 1,051.2°C, the atmospheric temperature was 17°C, and the ground temperature was 27°C. Here the lava specific enthalpy is calculated by its temperature taking thermal capacity and latent heat into account (Hidaka et al. 2005). The lava properties and

Table 1 Parameters for the 1986 Izu-Oshima LC-I lava flow simulation

Parameters	
Density	2.5×10^3 kg/m^3
Heat capacity	8.4×10^2 J/kg K
Thermal conductivity	1.56 W/m K
Latent heat of fusion	3.2×10^5 J/kg
Solidus temperature	1,000°C (1,273°K)
Liquidus temperature	1,100°C (1,373°K)
Specific enthalpy of solidus	1.07×10^6 J/kg
Specific enthalpy of liquidus	1.39×10^6 J/kg
Solidification fraction of liquidity loss	0.5
Specific enthalpy of liquidity loss	1.23×10^6 J/kg
Lava emissivity	0.66
Temperature of liquidity loss	1,050°C (1,323 K)
Extrusion rate	1.1×10^5 kg/s (0–3,600 s) 0 kg/s (>3,600 s)
Lava specific enthalpy	1.23×10^6 J/kg
Extrusion temperature	1,051.2°C (1,324.2 K)
Viscosity	5.0×10^3 Pa s
Atmospheric temperature	17°C (290 K)
Ground temperature	27°C (300 K)

physical parameters for the simulation are summarized in Table 1.

Figure 1c depicts the final thickness of a simulated lava flow. The overall features of the distribution fit the observed inundated area well. The flow runs rapidly down along the channel for about half an hour, then encounters flatter areas where the spreading velocity decreases. A thick part around the head of the flow exists from about 20 min and becomes significant after an hour, when the flux is slowing. Finally, the thickest part (exceeding 5 m) appears at the front of the flow. The simulated flow is faster than the observed lava flow of LC-I (Fig. 1b) since the simulated flow reached the point where the actual lava arrived at around 1900 LT (1 h after the beginning of the eruption) in about half an hour, even though the final distribution is well matched. The actual lava flow from the C6 crater also had more complex relationships with the opening of other craters and other factors. The small branch in the upper area is not significant for the actual lava flow because this area overlaps ejected ash falls, scorias, and new vents. The details are covered in the Discussion section. As a whole, this formulation generally reproduced the features of the LC-I lava flow; we use this result as a reference for the following simulations.

Artificial barrier effect

Using the numerical simulations we have developed, we can evaluate the effects of artificial barriers. The objective of these barriers is to reduce the length and area of inundation along with the velocity and temperature of the

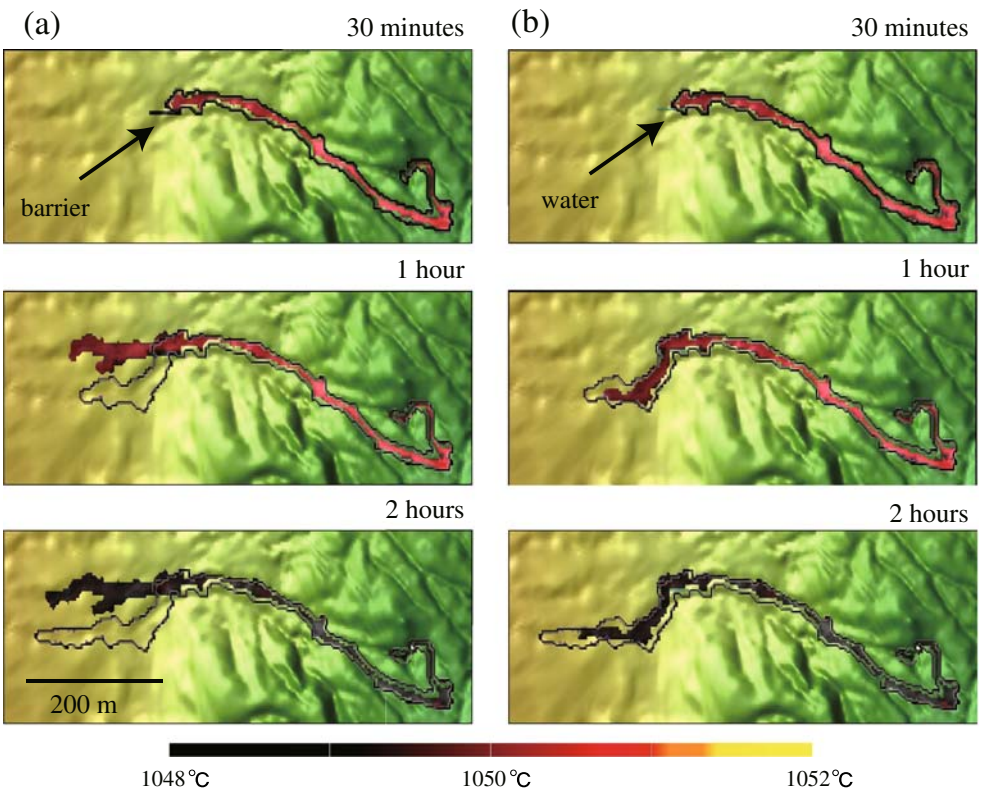

Fig. 2 **a** An example of simulated lava flow using an artificial barrier. The color shows the temperature at the surface of the lava. The size of the barrier is 130 m×20 m×10 m and is able to change the direction of lava flow. **b** An example of simulated lava flow using a water-cooling pool. The total amount of the water is 3.9×10^3 m^3. The solid boundary lines indicate the inundated area of the normal simulation in Fig. 1c

lava. Figure 2a is an example in which a barrier measuring 130 m (length)×20 m×10 m is placed at the point where the flow turns sharply southward. This barrier is partly successful in changing the direction straight to the west. The flow arrives at this barrier after one hour and cannot go further southward, running instead along the barrier, and accumulating lava at the boundary. The lava in front of the barrier is thicker than that for the no-barrier case, demonstrating that an artificial barrier can reduce the flow velocity and promote solidification and accumulation of lava, which then becomes a further obstacle. The final lava flow pattern is completely different from that with no barrier, and the total inundated area is about 97% of the no-barrier case.

Water-cooling effect

The effect of water spray was also quantitatively evaluated. In LavaSIM, we assume the distribution of water meshes and calculate heat flux between lava and water (Hidaka et al. 2005). Figure 2b depicts the temporal evolution of a lava flow with water cooling by 26 water blocks, each 10 m× 10 m×1.5 m, placed at the same location used for the barrier in the previous simulation. The total amount of water was 7.85×10^4 m^3. This estimate is about four times that by Hidaka (2004), which sprays water at the area where flow is more stagnating and the water-cooling is more effective. This is as much as the half of the total volume of lava flow LC-I, 1.6×10^5 m^3(Nagaoka 1988). In about 30 min, the flow arrives at the water-cooling area, and the temperature at the front is reduced (Fig. 3). This becomes very clear after 40 min, when there is a low-temperature area along the water-cooling barriers. The flow passes by the water to the south, since this part is lower than the other part. Along this overflow channel, there is a cooled edge on both sides, choking the flow. The final distribution of the lava flow indicates that the direction is not so different from that of the no-water-cooling case, but the length is decreased significantly.

Guiding channels effect

The third example is the effect of artificial channels dug to change the direction of lava flow (Fig. 4). This direction basically follows the topography of ground; therefore, once we introduce some guiding channels, the stream will go down toward them. Here we introduce two examples of simulations; (a) a perpendicular channel of 30 m width is set to bend the flow toward south in front of the originally bending area, and a parallel channel of 20 m width is found in the northern edge of the original inundated area to go straight toward the west; (b) a channel is set at the midpoint of the flow to lead the flow toward another valley nearby.

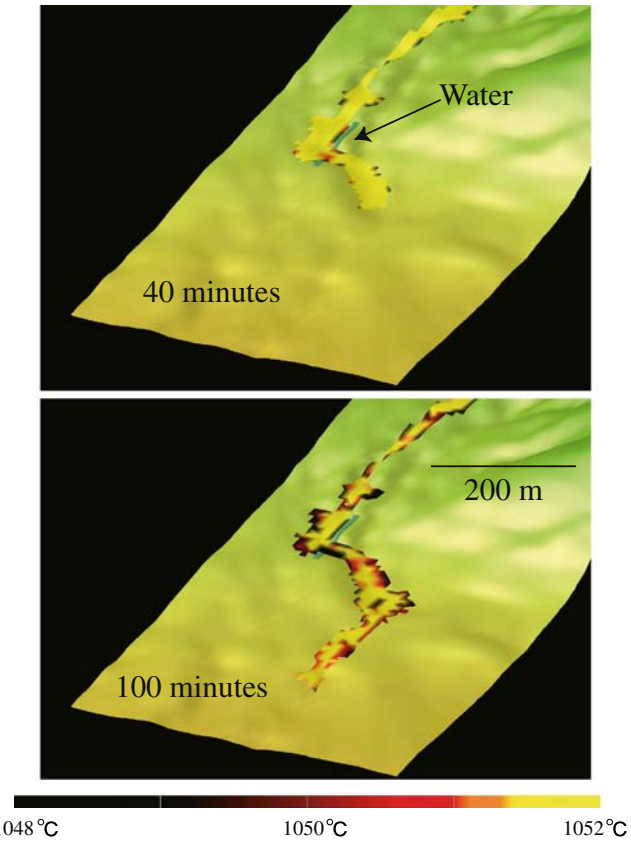

Fig. 3 Magnified lava flow pattern of the water-cooling simulation. The color in the lava flow distribution indicates the temperature of each area. Lava is cooled by the water at the margin of the flow. The water cooling effect controls the widths of lava flow and its distribution

The depths of these channels are assumed to be 5 m beneath their original altitudes. We placed these channels at relatively flat areas so that the channels may give the best results. The result of the simulation (a) shows that the channel successfully bypasses the flow toward the south and west, even though the final distribution of the lava-inundated area is not so different from the original (Fig. 1c). The result of simulation (b) works well to bend the flow toward the neighboring valley, and some portion of the emitted lava filled this valley. The final length of the inundated area is shorter than that of the original.

Discussion

The effects of barriers, water cooling and the guiding channels on the total area inundated are summarized in Fig. 5. The simulation of protection barriers indicates that a barrier is more effective when placed where the topography is more or less flat and the flow spreads out. In addition, a barrier almost parallel to the flow, that is, a barrier with a low angle to the lava flow stream, is more successful than a

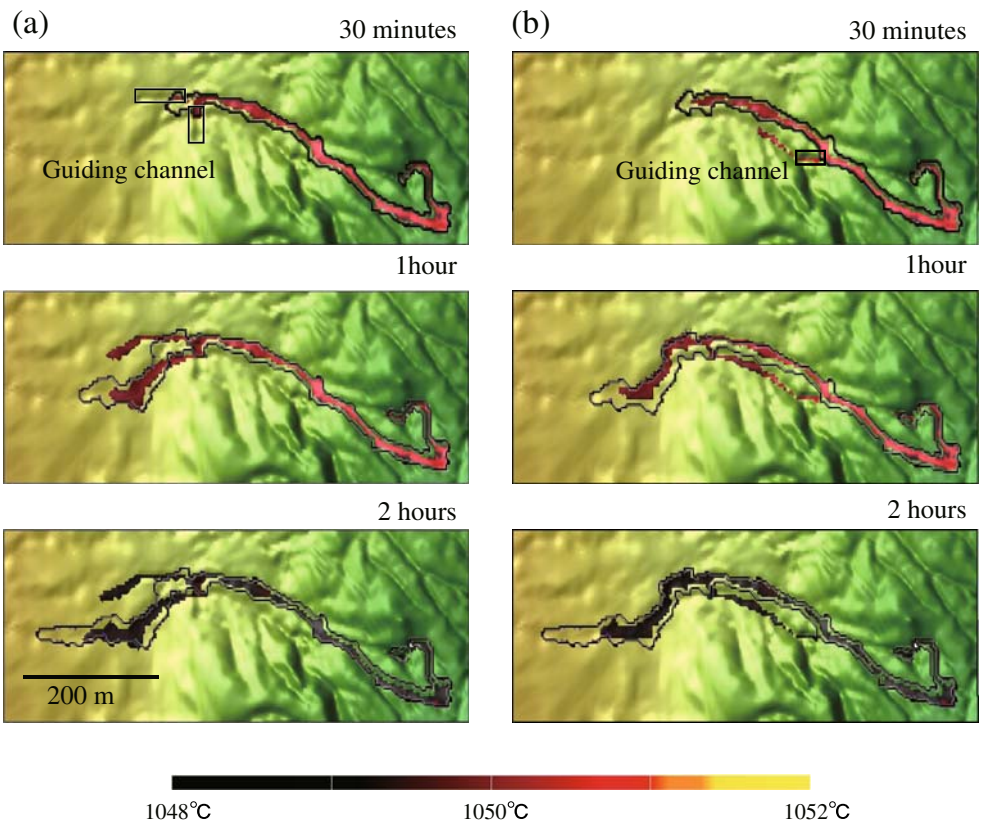

Fig. 4 Simulations using guiding channels to control lava flow. **a** Two guiding channels successfully divide the original flow into two valleys, and the final distribution is shorter than the original. **b** A guiding channel is used to bypass the flow into a neighboring valley to the south. Finally the branch merges into the original one

perpendicular barrier that we had made for a preliminary simulation. In Fig. 6, the effect of a barrier is shown as the distribution of the thickness of inundated lava. A barrier placed perpendicular to the flow prevents flow at first, but lava begins to accumulate in front of the barrier. When the following lava flow is thick enough, the accumulated lava causes it to pass over the barrier, as well as to both sides. The final distribution is not so different from the case with no barriers. The water-cooling simulation indicated about a 10% reduction in the total inundated area. In this case, we needed as much as 10^5 m^3 of water, which is impractical, especially in an emergency. Water spray is more effective considering that the lava surface has cracks and the effective cooling surface is several times larger than that of our formulation (Neri 1988). When water is poured onto the lava surface, the water intrudes through the cracks, further promoting the cooling effect.

The effect of guiding channels is closely related to the topography and works well for a shortcut or bypass; however, the flow itself is mainly governed by the topography as well as the emission rate, so we generally can control the direction of lava only in local regions. In some cases, the final distribution of lava may change downstream.

The misfit of the temporal length evolution between our simulation and observation occurs because the simulated flow is much faster than the actual flow, although the final

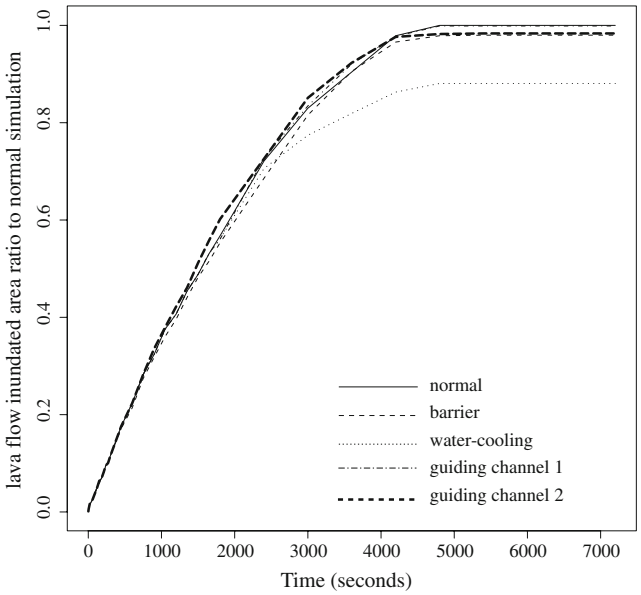

Fig. 5 Temporal changes of lava flow inundated area ratio compared with the normal simulation in Fig. 1c. *Solid line*: normal simulation (Fig. 1c); *dashed line*: barrier simulation (Fig. 2a); *dotted line*: water-cooling simulations (Fig. 2b). The barriered simulation shows the final distribution is about 97% of the normal simulation, while the water-cooling simulation is about 89% of the normal simulation. The barriered flow shows the inundated area decreases around 2,000 s, suggesting the lava accumulates at the front area of the barrier, but then it overcomes and/or goes toward the side of the barrier, and the final area is not so different. Two guiding channels simulations have similar effect to the barrier

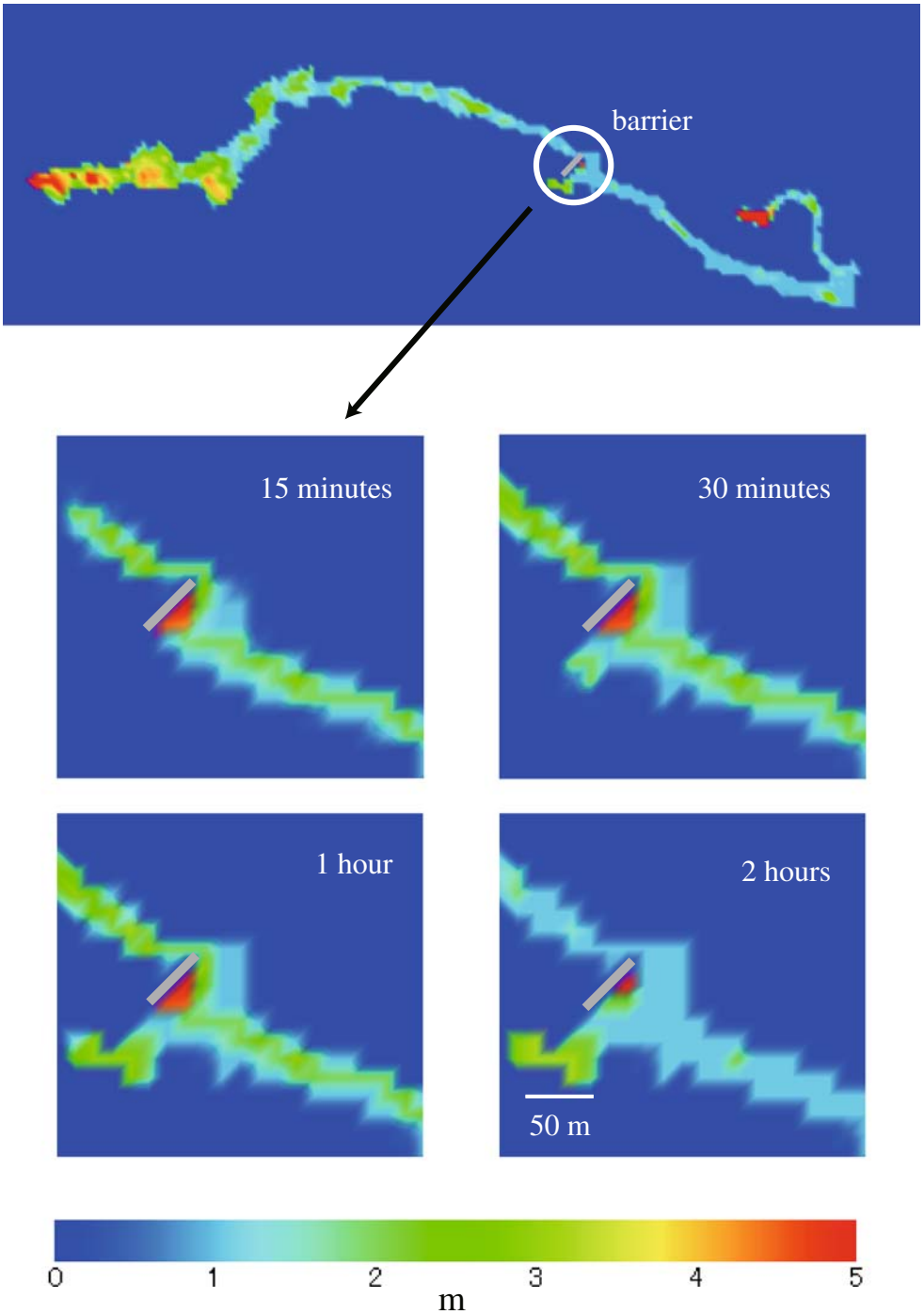

Fig. 6 Effect of a barrier placed perpendicular to lava flow. When lava reaches the barrier, it accumulates at the front of the barrier. After a while, some parts of the flow go over the barrier while other parts flow around the barrier. The final distribution is not so different from the original distribution shown in Fig. 1

distribution of lava-inundated areas is almost the same. We assumed the viscosity of magma to be equal to 5.0×10^3 Pa s based on the final distribution. To reduce the flow velocity, we would have to choose a higher viscosity, but this would reduce the final length of the lava flow, causing additional misfits. Temporal changes in viscosity due to temperature represent a key aspect of controlling the lava flow pattern. Viscosity and yield strength of lava increase associated with crystallization due to cooling and the degassing (Cashman et al. 1999; Umino et al. 2006; Umino 2007; Lipman and Banks 1987). LavaSIM can also formulate this physical model based on Goto's model (Goto et al. 1997), although this does not give a significantly different result. From the viewpoint of lava flow width, the lava flow is basically controlled by the topography, but the misfit here suggests the importance of lateral flow. In LavaSIM, the solidified lava crust moves only vertically (Hidaka et al. 2005), but in actual lava flows, the crust also moves horizontally, behaving as a barrier itself and reducing the effective viscosity. Artificial

barriers and water cooling will control the flow patterns in relation to these inherent obstacles, and the effective viscosity will be reduced. The next step in our lava-flow simulation is to include these effects in order to generate more realistic estimates for lava-control trials.

Conclusions

We evaluated the effects of barriers and water-cooling in controlling lava flow, applying them to lava flow LC-I, observed during the 1986 Izu-Oshima eruption. Our conclusions are as follows. (1) A barrier is effective in changing the path of the lava flow, especially when it is placed parallel to the flow in a flat area. (2) A barrier perpendicular to the flow initially stops the flow, but lava is accumulated in front of the wall, eventually allowing successive lava to overtop the barrier and bypass it. (3) Water-cooling is effective in diverting and controlling a lava flow, but requires a large volume (10^4 m^3). (4) Water-cooling enhances the solidification of the edge of the flow, choking the flow and reducing the final inundated area. (5) Guiding channels are effective to bypass the stream to protect local regions, taking the original topography into account.

Acknowledgements We are grateful to Mie Ichihara and Takeshi Nishimura who developed the lava flow simulation LavaSIM. Mauro Coltelli, Maria Marsella and Cristina Proietti provided useful comments on the cooling effects of fractures on the lava surface. Comments by Antonio Costa, Setsuya Nakada and John Stix were very helpful to improve our manuscript. We also acknowledge Momoe Nakamura for her kind support.

References

Barberi F, Carapezza M (2004) The control of lava flows at Mt. Etna. In: Bonaccorso, Calvari S, Coltelli M, Del Negro C, Falsaperla S (eds) Mount Etna: volcano laboratory. Am Geophys Union Geophys. Mon 143:357–369

Barberi F, Carapezza M, Valenza M, Villari L (1993) The control of lava flow during the 1991–1992 eruption of Mt. Etna. J Volcanol Geotherm Res 56:1–34

Cardaci C (2004) Lava flow diversions at Etna, the experiences of Department of Italian Civil Protection—technical aspects and socio-legal problems. Proceedings of International Symposium on Lava Flow Control and Disaster Mitigation, Fuji-Yoshida, Japan, pp 103–113

Cashman KV, Thornber C, Kauahikaua JP (1999) Cooling and crystallization of lava in open channels, and the transition of pahoehoe lava to 'A'a. Bull Volcanol 61:306–323

Costa A, Macedonio G (2005) Computational modeling of lava flows: a review. In: Manga M, Ventura G (eds) Kinematics and dynamics of lava flows. Geol Soc Am Spec Pap 396: 209–218

Crisci GM, Rongo R, Gregorio SD, Spataro W (2004) The simulation model SCIARA: the 1991 and 2001 lava flows at Etna. J Volcanol Geotherm Res 132:253–267

Endo K, Chiba T, Taniguchi H, Sumita M, Tachikawa S, Miyahara T, Uno R, Miyaji N (1988) Tephrochronological study on the 1986–1987 eruption of Izu-Oshima Volcano, Japan (in Japanese with English abstract). Bull Volcanol Soc Jpn 33:S32–S51

Favalli M, Pareschi MT, Neri A, Isola I (2005) Forecasting lava flows paths by a stochastic approach. Geophys Res Lett 32:L03305, doi:10.1029/2004GL021718

Geographical Survey Institute (2006) Land condition map of volcano, Izu Oshima

Goto A, Maeda I, Nishida Y, Oshima H (1997) Viscosity equation for magmatic silicate melts over a wide temperature range. Paper presented at Unzen International Workshop: Decade Volcano And Scientific Drilling. Univ Tokyo, Shimabara, Japan, pp 100–105

Hayakawa Y, Shirao M (1998) November 21–21, 1986 Izu Oshima 2B lava flows. Bull Volcanol Soc Jpn 33:S77–S90

Hidaka M (2004) Numerical simulation for lava flows. Proceedings of International Symposium on Lava Flow Control and Disaster Mitigation, Fuji-Yoshida, Japan, pp 77–89

Hidaka M, Goto A, Umino S, Fujita E (2005) VTFS project: development of the lava flow simulation code LavaSIM with a model for three-dimensional convection, spreading, and solidification. Geochem Geophys Geosys 6:Q07008, doi:10.1029/2004GC000869

Ishihara K, Iguchi M, Kamo K (1988) Reproduction of the 1986 Izu-Oshima lava flows by a numerical calculation (in Japanese with English abstract). Bull Volcanol Soc Jpn 33:S64–S76

Kauahikaua J (2004) History and technology of lava flow control attempts for Hawaiian eruptions. Proceedings of International Symposium on Lava Flow Control and Disaster Mitigation, Fuji-Yoshida, Japan, pp 3–16

Lipman PW, Banks NG (1987) Aa flow dynamics, Mauna Loa, 1987. US Geol Surv Prof Pap 1350:1527–1567

Nagaoka M (1988) Geomorphological characteristics of volcanic products of the 1986 eruption of Izu-Oshima volcano and its volume measured by photogrammetry. Bull Volcanol Soc Jpn 33: S7–S15

Neri A (1988) A local heat transfer analysis of lava cooling in the atmosphere: application to thermal diffusion-dominated lava flows. J Volcanol Geotherm Res 81:215–243

Siguresirsson T (1997) Lava cooling. In: Williams RS Jr (ed) Lava-cooling operations during the 1973 eruption of Eldfell volcano, Heimaey, Vestmannaeyjar, Iceland. US Geol Surv Open-File Rep 97-724

Umino S (2007) Characteristic of lava flows of Fuji volcano. Fuji Volcano. Yamanashi Institute of Environmental Sciences, Fuji-Yoshida. Volcanol Soc Japan, pp 269–283

Umino S, Nonaka M, Kauahikaua J (2006) Emplacement of subaerial pahoehoe lava sheet flows into water: 1990 Kupaianaha flow of Kilauea Volcano at Kaimu Bay, Hawai`i. Bull Volcanol 69:125–139

Vassale R (1994) The use of explosive for the diversion of the 1992 Mt. Etna lava flow. Acta Vulcanol 4:173–177

Wadge G, Young P, McKendrick I (1994) Mapping lava flow hazard using computer simulation. J Geophys Res 99:489–504